Chin. J. Astron. Astrophys. Vol. 4 (2004), No. 5, 415–426
(http://www.chjaa.org or http://chjaa.bao.ac.cn)

Chinese Journal of Astronomy and Astrophysics

SDSS J022119.84+005628.4: A Radio-Loud Narrow-Line Seyfert 1 Galaxy with Star Formation in its Nucleus *

Jing Wang[1,2], Jian-Yan Wei[2] and Xiang-Tao He[1]

[1] Department of Astronomy, Beijing Normal University, Beijing 100875; wj@bao.ac.cn
[2] National Astronomical Observatories, Chinese Academy of Sciences, Beijing 100012

Received 2004 March 2; accepted 2004 June 28

Abstract The optical spectrum of SDSS J022119.84 + 005628.4 (R. A. = $02^{\rm h}$ $21^{\rm m}$ $19.84^{\rm s}$, Dec = $00^\circ56'$ $28.4''$, J2000; $z = 0.399785 \pm 0.000558$) is analyzed by multi-component profile modelling. The small flux ratio of $[{\rm O\,III}]_{\rm NC}/{\rm H}\beta$ (=0.78) and FWHM(H$\beta_{\rm BC}$) = 1778.1 ± 85.9 km s^{-1} led us to identify SDSS J022119.84 + 005628.4 as a Narrow-line Seyfert 1 galaxy with RFe= $1.4^{+1.0}_{-1.0}$ and intermediate radio loudness, $\log R = 1.93$. The continuum low jump at the Balmer limit might be contributed by a starburst component, which suggests that the object is a relatively young AGN with star-formation activity in its inner region. This provides a useful observational test of the AGN evolution. The low flux ratio of the narrow components, $[{\rm O\,III}]/{\rm H}\beta = 1.62$, and the prominent $[{\rm O\,II}]\lambda3727$ emission, $[{\rm O\,II}]/[{\rm O\,III}] = 2.24$, suggests that there should be a group of AGNs different from Seyfert 2s when their broad line regions are obscured by the torus on the line of sight. A possible orientation effect is suggested to interpret the observed Seyfert 1.5s-like spectrum of the object. The spectrum features prominent broad blue wings of both $[{\rm O\,III}]\lambda\lambda4959$ and 5007. After excluding other possible contributions, we conclude that the broad components are emitted by [O III] itself. The material emitting the broad [O III] line is probably situated in a transient line region (with a low electron density, $n_{\rm e} < 10^7{\rm cm}^{-3}$) between the broad line region (BLR) and the narrow line region (NLR). The object can be classified as a "blue outlier" defined by Zamanov et al., according to its velocity shift $\upsilon_r([{\rm O\,III}]) = -293.6 \pm 18.0$ km s^{-1}, relative to the systematic velocity.

Key words: galaxies: active — galaxies: Seyfert — quasars: individual (SDSS J022119.84 + 005628.4)

1 INTRODUCTION

Narrow-line Seyfert 1 galaxy (NLS1) defined by Osterbrock & Pogge(1985) is an important special sub-class of active galactic nucleus (AGN). Subsequent observations indicate that NLS1s

* Supported by the National Natural Science Foundation of China.

are not infrequent in the universe. They amount to about 15% and 30% to 50% in selected hard and soft X-ray AGN samples, respectively (Stephens 1989; Puchnarewicz et al. 1992; Grupe et al. 1999). There are two effective criteria in the optical band for picking up the NLS1s from the whole family of Seyfert galaxies. 1) Although the NLS1s resemble the BLS1s (broad line Seyfert 1s) in the shape of the continuum, the Balmer permitted emission lines, usually with FWHM(Hβ) $< 2000\,\mathrm{km\ s^{-1}}$, are a little broader than the forbidden lines. 2) Weak [O III] lines with [O III]λ5007/H$\beta < 3$ (Osterbrock & Pogge 1985; Pogge 2000). In addition, most of the NLS1s are characterized by strong Fe II complex as well as soft X-ray excess (e.g. Boller et al. 1996; Brandt, Mathur & Elvis 1997; Vaughan et al. 1999a; Leighly 1999b; Reeves & Turner 2000). To interpret the peculiar nature of the NLS1s, many authors believed that NLS1s possess small black hole masses and high accretion rates, relative to the Eddington accretion limit (e.g. Boller et al. 1996; Laor et al. 1997; Pounds, Done & Osborne 1995; Kuraszkiewicz et al. 2000; Pounds & Vaughan 2000; Wandel 2000).

To answer the question 'what determines the accretion rate in the AGNs', Mathur (2000) showed that NLS1s might be Seyfert galaxies in their early stage of evolution. The evolutionary scenario is supported by the bright IR emission, by super-solar gas phase metallicities, by analogy with high-redshift quasars and by an accretion rate closing on the Eddington limit. The high accretion rate provides a large amount of gas that can sustain the violent activity in the nucleus. Therefore, as pointed out by Mathur (2000), searching for starburst components in NLS1s may provide a suggestive clue for the starburst-NLS1 connection. Although some encouraging results have been derived from the observations of individual objects, notably, the identification of a surrounding circumnuclear starburst ring in I Zw1, the prototype NLS1, by near IR and CO mapping (Schinnerer et al. 1998), no conclusive statistical evidence has been obtained. Thus, searching for NLS1s with signs of star formation remains crucial for verifying above hypothesis.

It has been pointed out that there is a correlation between the black hole mass and radio power. Laor (2000) reported a dichotomy in the radio loudness distribution of PG quasars, namely, nearly all objects with $M_{\rm BH} > 10^9 M_\odot$ are radio-loud while those with $M_{\rm BH} < 3 \times 10^9 M_\odot$ are practically radio-quiet. If this is true, a more massive black hole should have been acquired to inhabit the center of a radio-loud NLS1 (RL NLS1). Thus, radio-aloud and radio-quiet NLS1s differ in the mass of the central source. Even if NLS1s are generally radio quiet objects, tens of RL NLS1s have been discovered in recent years. Whalen et al. (2001) found 20 more RL NLS1s from the First Bright Quasar Survey (FBQS) in a sample of 62 radio-selected NLS1s with a $\sim 40\%$ detection rate. In addition, over a dozen of RL NLS1s have been identified (Remillard et al. 1986; Siebert et al. 1999; Grupe et al. 2000; Zhou & Wang 2002; Zhou et al. 2003) with medium radio intensity for most of them. We are thus prompted to ask the questions, "Is there surely a more massive black hole in RL NLS1s than in radio-quiet NLS1s?" , "Why are RL NLS1s so infrequent?". Both these questions should be addressed. Despite the tiny fraction of RL NLS1s, their detection and physical exploration are of great significance for understanding the AGNs.

In this paper, we report the discovery of an intermediate RL NLS1, SDSS J022119.84 + 005628.4, with a detected Balmer jump and prominent broad and blue-shifted components of [O III]$\lambda\lambda$4959, 5007, from the Data Release 2(DR2) of Sloan Digital Sky Survey (SDSS). The spectral analysis is presented in Sect. 2. We clarify the results of profile fitting in Sect. 3. A discussion is given in Sect. 4.

2 SPECTRAL ANALYSIS

The optical spectrum of SDSS J022119.84+005628.4 (R.A.= $02^{\rm h}21^{\rm m}19.84^{\rm s}$; Dec= $00°56' 28.4''$, J2000; $z = 0.399785 \pm 0.000558$) was observed on 2000 September 30 by the SDSS 2.5 m telescope at Apache Point Observatory, New Mexico. The spectrum covers the range 3800 – 9200Å with resolution 1800 (Schneider et al. 2002) was obtained with an exposure of 2700 s. The spectral quality is medium, with S/N ratio $\sim$ 13, according to DR2. Figure 1 presents the unprocessed spectra. Some prominent emission lines have been marked.

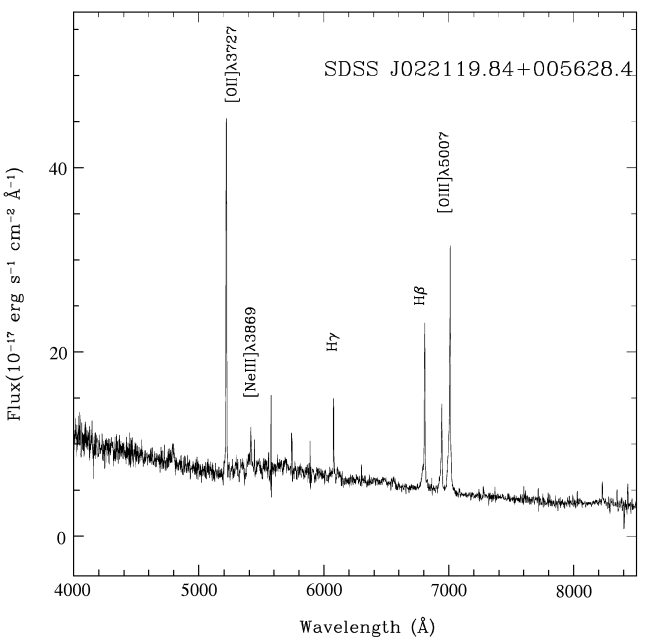

Fig. 1 Unprocessed spectrum of SDSS J022119.84+005628.4. The prominent emission lines are marked.

The extracted spectrum is reduced by following steps: (1) The Galactic extinction is corrected by $E(B-V) = 0.036$ mag, from NED, assuming an $R_V = 3.1$ extinction curve. (2) De-redshift the spectrum according to the narrow peak of Hβ along with the K correction. (3) Attempting to estimate the flux of Fe II in the optical band, we remove the weak Fe II complex using the commonly accepted templates in Boroson & Green(1992). Here, a successful Fe II removal results in a flat continuum between Hγ and Hβ and in the range 5100–5400Å. Although the precise removal and an accurate value of the flux of Fe IIλ4570 cannot be done by eye in SDSS J022119.84+005628.4, we conclude that the flux measured between rest wavelengths 4434Å and 4684Å, is about 3.25×10^{-15} erg s^{-1}cm^{-2}Å^{-1}, corresponding to RFe = $1.4^{+1.0}_{-1.0}$ (RFe is defined as the flux ratio of Fe II to Hβ). The upper and lower limits are obtained by careful iterative experiments with a series of values of the flux of the Fe II template. Outside of the limits, the Fe II subtracted continuum is absolutely unacceptable. The Fe II removal is sketched

in Fig. 2. The Fe II subtracted and blended spectra are graphed by the middle and upper curves, respectively, offset upward by an arbitrary amount for better visibility. The best removed Fe II complex, RFe = 1.4, is shown by the bottom curve, (4) The Fe II contamination-removed profile is modeled by the multi-component fitting task SPECFIT (Kriss 1994) in the IRAF-STSDAS package, specifically, 1) the continuum is fitted by a power law basing upon the selected wavelength windows 4500–4600Å and 5100–5500Å in the rest frame. 2) For the prominent reflection of profiles of Hβ and [O III]$\lambda\lambda$4959,5007, two Gaussian profiles, a narrow core superposing on a broad and blue shifted base, must be used to reproduce each of the observed profiles by means of χ^2 minimizing. The atomic physics relations, $F_{5007}/F_{4959} \doteq 3.0$ (Storey & Zeippen 2000) and $\lambda_{4959}/\lambda_{5007} = 0.9904$, are used for decreasing the number of free parameters in the modelling of both the narrow and broad components. The modelling is shown schematically in Fig. 3. It is important to stress that the profiles of Hβ and [O III] can be fitted very well by two Gaussian profiles, because the adequate S/N ratio and the prominent reflection in the profiles neatly separate the narrow core and the blue-shifted base. The goodness of the fit is indicated by the low residuals, shown in the bottom panel of Fig. 3, in the whole Hβ and [O III] regions.

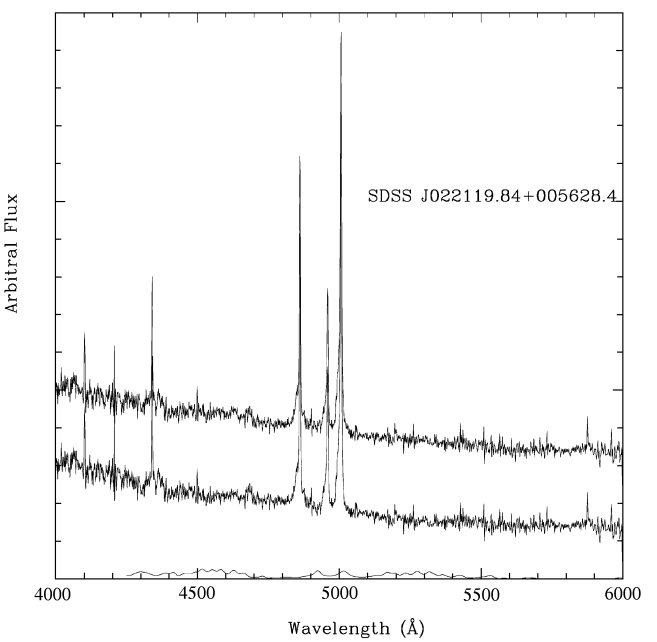

Fig. 2 Removal of the Fe II complex. The bottom curve is the removed Fe II complex, with RFe = 1.4. The Fe II blended spectrum is shown by the upper curve, shifted upward for visibility. The middle curve is the Fe II subtracted spectrum.

3 RESULTS

We tabulate the results of profile fitting in Table 1. The flux of each component is conveniently normalized by that of the narrow core of Hβ denoted as H$\beta_{\rm NC}$.

Table 1 Results of Multi-component Profile Fitting of SDSS J022119.84+005628.4

Components	Normalized Flux[a]	λ^{b}_{peak}	FWHM[c]
$H\beta_{NC}$	1.00.....	4861.1 ± 0.1	253.9 ± 7.1 ....
$H\beta_{BC}$	1.09 ± 0.05	4856.8 ± 0.6	1778.1 ± 85.9
[O III]$\lambda5007_{NC}$	1.62 ± 0.06	5006.4 ± 0.1	298.1 ± 6.3 ....
[O III]$\lambda5007_{BC}$	1.83 ± 0.07	5001.5 ± 0.2	1263.5 ± 31.0
[O II]$\lambda3727$[d]	3.63 ± 0.13	3727.6 ± 0.1	445.2 ± 2.4 ....

[a] The flux of each component is relative to that of $H\beta_{NC}$, here $F(H\beta_{NC}) = (2.13\pm0.06)\times10^{-15}$ erg s^{-1} cm^{-2};
[b] The wavelength, in units of Å, refers to the peak of the profile;
[c] In units of km s^{-1};
[d] The emission line [O II]$\lambda3727$ is measured by direct integration.

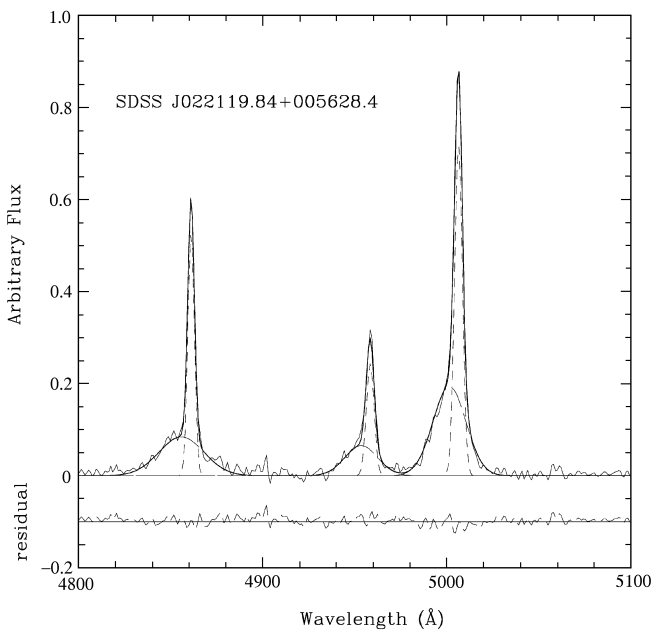

Fig. 3 Fitting of the continuum-removed profile by χ^2 minimizing. The modeled composite profile is shown by the stick solid line. The narrow and broad components of Hβ and [O III] are given by the short and long dashed line, respectively. The lower panel plots the residuals in the wavelength range 4800–5100Å.

From Table 1, we obtain two strong pieces of evidence for SDSS J022119.84 + 005628.4 being an NLS1, with $M_B = -22.1$mag (assuming with DR2, $\Omega_0 = 1$, $H_0 = 50$ km Mpc^{-1} s^{-1}). First, the flux ratio of the narrow [O III]$\lambda5007$ to the total Hβ([O III]$_{NC}$/Hβ) is only 0.78, only about 1/4 of the upper limit for Seyfert-1 (Osterbrock & Pogge 1985). Such a weak [O III] emission excludes the possibility of it being a Seyfert-2, which usually has [O III]$\lambda5007$/H$\beta \geq 3$, and mostly is larger than 5 (Veilleux & Osterbrock 1987). Secondly, the FWHM of the broad Hβ line is 1778.1 ± 85.9 km s^{-1}, which satisfies the condition of Serfert-2, FWHM(Hβ) < 2000 km s^{-1}.

SDSS J022119.84+005628.4 (NVSS J022118+005628) was also observed in the radio band by NRAO VLA Sky Survey (NVSS) (Condon et al. 1998) with a flux of 3.7 ± 0.6 mJy at 1.4 GHz. The observation suggests that the object is an intermediate radio loud AGN with a radio loudness, log R equal 1.93 (> 1). Here, the loudness R is defined as the flux ratio of radio to optical at λ4400 (Kellermann et al. 1989). The optical flux at λ4400, $S_{\rm o}$, in units of mJy, is assessed by the formula $B = -2.5 \log S_{\rm o} + 16.64$ (Schmidt & Green 1983), B (=20.05 mag) being the apparent magnitude at B band, obtained from the SDSS photometric system with $g^* = 19.594$ mag and $r^* = 18.996$ mag (Fukugita et al. 1996).

Figure 4 presents a real detected Balmer discontinuity in the spectrum of SDSS J022119.84 + 005628.4, which separates the continuum into two parts. The continuum declines blueward of [Ne III]λ3869 and joins to another part blueward of [O II]λ3727 with a flux decrease about 3.7×10^{-17} erg s^{-1}cm^{-2}Å^{-1}. For the narrow and faint absorption of Ca II H K at $\lambda\lambda$3934, 3968, we suppose that the low jump of continuum should be attributed to a mixture of high order Balmer absorption lines and the absorption at Balmer limit, systematically redshifted. The Balmer jump indicates a component of star formation in the nucleus of the object.

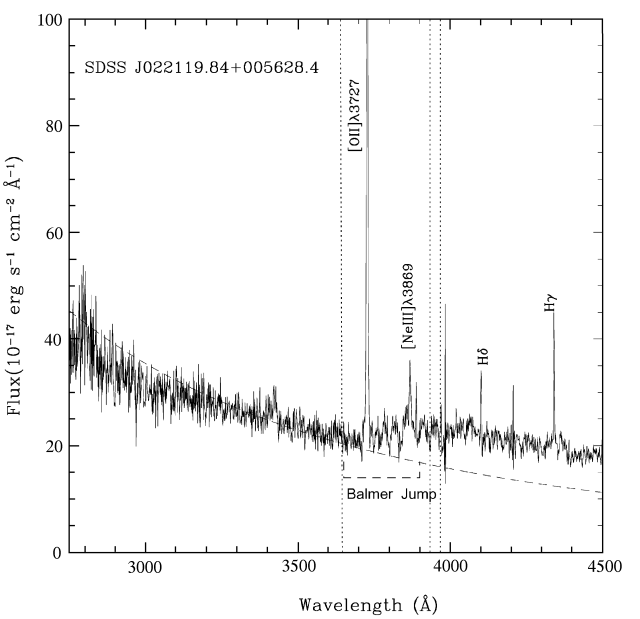

Fig. 4 Balmer jump in the spectrum of SDSS J022119.84+005628.4. The prominent emission lines are marked as in Fig.1. The short dashed vertical lines mark the Ca IIH K absorptions and the Balmer limit. The long dashed line marks the modeled continuum blueward of the Balmer discontinuity.

The other prominent spectral features are the broad and blue-shifted components of [O III] $\lambda\lambda$ 4959, 5007 and Hβ. Unlike most previous researches, we were able to easily decompose the profile and make accurate measurements with its appropriate spectral resolution and obvious reflection of the profiles. The flux ratio of the broad-to-narrow components of Hβ is 1.09 ± 0.05. In [O III] over half of the flux is contributed by the broad component with $[\mathrm{O\,III}]_{\rm BC}/[\mathrm{O\,III}]_{\rm NC} \sim 1.13$. A strong emission of $[\mathrm{O\,III}]_{\rm BC}$ is evidenced by a large normalized flux of 1.83 ± 0.07.

The FWHM of the broad [O III] line is 1263.3 ± 31.0 km s^{-1}, somewhat less than that of the broad Hβ line, FWHM(H$\beta_{\rm BC}$) $= 1778.1 \pm 85.9$ km s^{-1}. On the other hand, the broad [O III] is blue-shifted by about -4.9 ± 0.3Å with respect to its narrow core, corresponding to -293.6 ± 18.0 km s^{-1}. The blue-shift is about the same as that of the broad Hβ relative to the center of the narrow Hβ line, namely, -4.3 ± 0.6 Å or -265.4 ± 37.0 km s^{-1}. The spectrum is also features a weak He IIλ4686 as well as an intensive low-ionization emission of [O II]λ3727. The normalized integrated flux of [O II]λ3727 is as high as 3.63 ± 0.13 with [O II]/[O III]$_{\rm NC} = 2.24$, implying a low-ionization stage of the narrow emission. The inferred ionization parameter is $\log U \approx -3.1$ (Penston et al. 1990).

4 DISCUSSION

SDSS J022119.84+005628.4 was not identified as an NLS1 and so was not included in the sample of 150 NLS1s given in the Early Date Release(EDR) of SDSS edited by Williams et al. (2002). Their selection rule was a weak [O III] emission, an evident Fe II complex and no obvious broad components in Hβ and Hα. That this object was left out is likely due to its having a weak Fe II complex and a broad component of Hβ. We will address this issue further in Sect. 4.3.

4.1 SDSS J022119.84+005628.4: An NLS1 Amidst Starburst Activity

Basing upon a variety of evidence, Mathur (2000) suggested that NLS1s with a high accretion rate are relatively young AGNs and Seyfert galaxies in their early stage of evolution. To date, a great deal of favorable evidence has been obtained from observations. One line of evidence supporting this scenario is that NLS1s may have super-solar gas phase metallicities. In addition to the arguments listed in Mathur (2000) and Komossa & Mathur (2001), the over-abundance of NLS1s has also been revealed in more recent studies. Nagao et al. (2002) found systematic higher metallicities in NLS1s than in BLSy1s. Lately, the evidence for super-solar metallicities was found in Ark 564, a well known NLS1 (Romano et al. 2004). On the other hand, the morphological study of NLS1s statistically supported the evolutionary paradigm for NLS1s. The results indicated that large-scale stellar bars starting at ~ 1 kpc from the nucleus are much more common in NLS1s than in BLSy1s (Crenshaw et al. 2003, and reference therein). A more commonly disturbed environment of NLS1s can efficiently transfer gas into the inner region, fuelling the AGN's activity to close to its Eddington limit of accretion, and triggering off starburst. Detection of starburst components in NLS1s is a powerful evidence of the NLS1 evolution, as suggested by Mathur (2000). The composite spectra of SDSS J022119.84 +005628.4, containing a typical AGN spectrum and a low jump at the Balmer limit contributed by star formation and intensive low-ionization [O II] emission, imply that two power systems, AGN activity and star formation, are going on in the nucleus of the object. Here, the starburst found in NLS1, SDSS J022119.84+005628.4 provides us a favorable observational test for the AGN evolutionary scenario, although the identification is without detailed age diagnosis. The diagnosis depends on stellar population synthesis, evolution model of AGN and the technique of decomposition between the contribution of active and inactive components (e.g. Brotherton et al. 1999, 2002). It is, unfortunate that the decomposition as executed in Brotherton et al. (1999, 2002) was complicated by an inadequate S/N ratio, a poor spectral resolution and a lack of evident high order series of Blamer absorption. The question of decomposition will be addressed in future studies.

4.2 Narrow Emission of SDSS J022119.84+005628.4

Up to now, no consensus has been reached on the properties of the NLR of the NLS1s. Rodriguez-Ardila et al. (2000), from a Gaussian component analysis of the Hβ profile in seven NLS1s, suggested that the NLR, with a low-ionization stage and giving a [O III]λ5007/H$\beta_{\rm BC}$ ratio varying from 1 to 5, is different from that of the BLSy1s and Seyfert 2s with the ratio commonly estimated at 10. A contrary result, however, was obtained that the narrow forbidden line ratios of [O I]λ6300/[O III]λ5007 and [O III]λ4363/[O III]λ5007 are statistically alike for the NLS1s and BLSy1s (Nagao et al. 2001). This last result was obtained using a pair of diagnostic line ratios, [O III]λ5007/Hβ and [N II]λ6763/Hα, from the best single Lorentz profile modelling of the Balmer emission line profiles (Véron-Cetty et al. 2001). In practice, the accuracy of the results is mostly limited by the decomposition of the blended narrow and broad components of the permitted lines, especially in the NLS1s. Fortunately, here, the Hβ emission profile can be decomposed reliably by χ^2 minimization because of the adequate spectral resolution and, most important, the prominent reflection. For the low ratio of [O III]$_{\rm NC}$/H$\beta_{\rm NC}$($= 1.62 \pm 0.06$) and intensive emission of [O II]λ3727 with normalized flux as much as 3.63 ± 0.13, the ionization stage of material emitting narrow lines is much lower than that observed in Seyfert 2s and BLSy1s. The result gives us a hint that there should be a type of AGNs that has a much lower ionization stage of narrow emission than usual and cannot be identified as Seyfert 2s when their broad line regions (BLRs) are obscured by the torus on the line of sight.

The physical condition of the NLR of SDSS J022119.84+005628.4 is potentially more like that of Low Ionized Nuclei Emission Region (LINER) or H II region. The absence of most useful diagnostic lines in the covered wavelength range, however, makes further identification difficult. We first suspected that the LINER could be a possible realistic counterpart of NLS1 with obscured BLR. On the other hand, the low stage of ionization could also be due to the degeneracy of radiation of the AGN and H II region, because of the identified nuclear starburst activity. In this case, to recover the genuine condition of the NLR of the AGN, a detailed decomposition into the AGN and star formation components should be performed. If so, we further speculate that the observed low ratio of [O III]$_{\rm NC}$/H$\beta_{\rm NC}$ in some NLS1s might have simply resulted from an admixture of contributions of AGN and starburst. It suggests that the ingredient of star formation in the AGN's nuclear region can be easily and roughly estimated by the low ratio of [O III]$_{\rm NC}$/H$\beta_{\rm NC}$ rather than the blurred Balmer jump in most cases.

4.3 Orientation Effect

In this section, we propose a plausible interpretation of the weak Fe II emission in SDSS J022119.84 + 005628.4. The detailed analysis of results indicates that the flux ratio of broad and narrow component is 1.09 for Hβ is 1.09, and 1.13 for [O III]. Because of the smaller proportion of broad component in Hβ than in [O III] and the weak Fe II complex, a majority of BLR with intensive Fe II complex and depressed [O III] emission might be obscured on the line of sight. Furthermore, a Seyfert 1.5s-like NLS1 is suggested for the object according to the flux ratio [O III]$_{\rm NC}$/H$\beta = 0.78$ (Osterbrock 1989; Winkler 1992). So far, even if the obscuring paradigm is postulated to explain the various properties of the AGN, the origin and maintenance of the obscuring material are still poorly understood. Recently, besides the classical obscuring torus, a number of lines of evidence show that starburst taking place in the nucleus can also obscure the central AGN's activity (e.g. Levenson et al. 2001). Fabian et al. (1998) proposed that the circumnuclear clouds boosted by supernovae (SNe) from starburst can obscure the central nucleus. In SDSS J022119.84 +005628.4, it is possible that the obscuration can be partially due

to the existence of starburst in its inner region.

4.4 Prominent Blue Wing and Outflow in TLR

The asymmetric profile of [O III] characterized by an extended wing blueward and a sharp falloff redward has been mentioned in early papers (Heckman et al. 1981; Vrtilek & Carleton 1985; Whittle 1985a; Veilleux 1991b). Véron-Cetty et al. (2001) found that, in general, a genuine narrow Gaussian component with FWHM $\sim 200 - 500$ km s^{-1} and a blue-shifted broad Gaussian component with FWHM $\sim 500 - 1800$ km s^{-1}, could rebuild the observed [O III] profile in a sample of 64 NLS1s. Recently, numerous sources whose [O III]λ5007 profiles can be separated into two components, a narrow unshifted core and a strong blue wing, were found for a sample of some 200 low-redshift AGNs (Zamanov et al. 2002).

4.4.1 The Identification of the Broad Wing of [O III]

The origin of the broad wing of [O III]λ5007 has remained an open question so far. Some authors interpreted the broad wing to come not only from the [O III] itself but also from a significant blend of Fe II(42)λ5018, He IIλ5016, S II$\lambda\lambda$5041, 5056 or even Hβ. Foltz et al. (1983) and Meyers & Peterson(1985) interpreted the broad wing in Akn 120 as a blending of the Fe II emission and a broad component of [O III]. Because of their weakness we can easily exclude Fe II complex and S II$\lambda\lambda$5041, 5056 as contributors to the [O III]. The contribution of He Iλ5016 can be excluded on the grounds that He IIλ4861 and He Iλ5876 are weak. Another strong piece of evidence, that [O III] blue wing in SDSS J022119.84 +005628.4 comes mainly from [O III] itself rather than the other candidates mentioned above, is that both [O III]$\lambda\lambda$ 4959 and 5007 have similar blue wings from the best modelling (see second paragraph in next section).

4.4.2 Where Is The Broad Wing From?

The observation of Seyfert galaxy Fairall 9 indicated that the broad wing of [O III] in this object is caused by high velocity material located far (no less than 1.3 pc) from the central source. Stirpe, van Groningen & de Bruyn (1989) found the shape of the spectrum remained unvaried over four years. Van Groningen & de Bruyn(1989) suggested that the emission region of the [O III] broad wing is located in the transition line region (TLR), between the BLR and NLR, with a low density ($n_{\rm e} \sim 10^6 {\rm cm}^{-3}$) and moving at several thousands km s^{-1}. Mason et al. (1996) examined the profiles of Hα, Hβ and [O III] in RE J1034+396, an X-ray selected AGN from ROSAT Wide Field Camera all-sky extreme-ultraviolet survey (Pounds et al. 1993; Pye et al. 1995; Shara et al. 1993; Mason et al. 1995) and gave the intermediate emission line region (ILR) a possible size of the order of 1 pc and an intermediate FWHM of ~ 1000 km s^{-1}. The photoionization calculation by Puchnarewicz et al. (1995) which reproduced the spectrum of RE JJ1034+396 very well indicated that the density of the ILR is on the order of $N_{\rm e} \sim 10^{7.5} {\rm cm}^{-3}$, which is much lower than the density of ordinary BLRs and higher than that of the NLRs.

The large FWHM value of the broad [O III] line, implying a corresponding lower electron density ($N_{\rm e} \sim 10^{6\sim7}$ cm^{-3}) in the inner NLR and the BLR, suggests that the broad [O III] should be possibly produced in the TLR. Moreover, as in the NLR emission, the atomic physical correlations, $F_{5007}/F_{4959} \doteq 3$ and $\lambda_{4959}/\lambda_{5007} = 0.9904$, successfully reproduce the observed blue wings of [O III]$\lambda\lambda$4959, 5007. The identical relationships suggest that in the TLR and NLR, identical physical processes are going on with different values for some parameters, such as electron density and/or the ionization parameter.

4.4.3 The Outflow

The character of outflow of TLR can be identified and explored by comparing the profiles of the blue wings of [O III] and Hβ. The blue-shift of the broad [O III] is approximately equal to that of Hβ ($\Delta v_r = 28.2 \pm 41.1$ km s^{-1}). On the other hand, the FWHM of Hβ is very much broader than that of [O III], the latter is ΔFWHM $= -514.6 \pm 91.3$ km s^{-1}. The difference implies that the outflow velocity is approximately kept a constant with the distance from the central source. Due to the velocity shift between the [O III] narrow and broad components, v_r([O III]) $= -293.6 \pm 18.0$ km s^{-1}, the object can be identified as a "blue outlier", an object with a blueshift amplitude of [O III] larger than 250 km s^{-1} (Zamanov et al. 2002).

5 CONCLUSIONS

In this paper we have analysed the optical spectrum of SDSS J022119.84+005628.4 by a multi-component fitting for Hβ and [O III] regions. From the results of the profile modelling, we find:

1. According to the small flux ratio of [O III]$\lambda 5007_{\rm NC}$/Hβ(=0.78) and narrow emission of Hβ(FWHM $= 1778.1 \pm 85.9$ km s^{-1}), SDSS J022119.84 + 005628.4 is an intermediate radio-loud ($\log R = 1.93$), NLS1 with RFe $= 1.4^{+1.0}_{-1.0}$, from the DR2 of SDSS. The small [O III]/Hβ ratio of their narrow components and the low-ionization emission of [O II]λ3727 show that the ionization stage of the narrow line emission of the object is obviously different from, and much lower than, that of Seyfert 2s. It argues for a different appearance of the AGN when its BLR is obscured in the line of sight.

2. The object provides us with a useful observational test for the AGN evolutionary scenario. The low jump in the continuum at the Balmer limit indicates that both nuclear activity and star formation are going on in the nucleus of SDSS J022119.84 +005628.4. The detected spectral signs of starburst give us a hint that the object is a relatively young AGN at an early stage of its evolution.

3. Effect of orientation is an alternative interpretation for the observed spectrum of SDSS J022119.84 + 005628.4. In this interpretation, we do not observe intensive Fe II complex because a large part of the BLR is obscured by the torus tilted at a large viewing angle.

4. The spectrum of SDSS J022119.84+005628.4 features prominent blue wings of [O III]$\lambda\lambda$4959, 5007 as well. We ascertain that the blue wings are mostly contributed by the the broad and blue-shift components of [O III] itself. The material emitting the broad [O III] should be situated in the TLR between the BLR and the NLR, with a low electron density ($n_{\rm e} < 10^7 {\rm cm}^{-3}$) and a prominent outflow velocity. The object is further identified as a "blue outlier" as defined by Zamanov et al. (2001).

Acknowledgements We are gratefully to an anonymous referee for many useful suggestion. This paper has benefited from his careful and critical review. We thank Dr. Xu Dawei, Wu Hong and Hao Caina for valuable discussion and help. This work was supported by the Ministry of Science and Technology of China, under grant NKBRSF G1999075404, and made use of the SDSS archive data, created and distributed by the Alfred P. Sloan Foundation.

References

Boller T., Brandt W. N., Fink H., 1996, A&A, 305, 53
Boroson T. A., Green R. F., 1992, ApJS. 80, 109
Brandt W. N., Mathur S., Elvis M., 1997, MNRAS, 285, 25
Brotherton M. S., van Breugel Wil., Stanford S. A., 1999, ApJ, 520, 87
Brotherton M. S., Grabelsky M., Canalizo G. et al., 2002, PASP, 114, 593
Condon J. J., Cotton W. D., Greisen E. W. et al., 1998, AJ, 115, 1693
Crenshaw D. M., Kraemer S. B., Gabel J. R., 2003, AJ, 126, 1290
Fabian A. C., Barcons X., Almaini O., Iwasawa K., 1998, MNRAS, 297, 11
Foltz C. B., Wilkes B. J., Peterson B. M., 1983, AJ, 88, 1702
Fukugita M., Ichikawa T., Gunn J. E. et al., 1996, AJ, 111, 1748
Grupe D., Beuermann K., Mannheim K., Thomas H. -C., 1999, A&A, 350, 805
Grupe D., Leighly K. M., Thomas H. -C., Laurent-Muehleisen S. A., 2000, A&A, 356, 11
Heckman T. M., Miley G. K., van Breugel W. J. M., Butcher H. R., 1981, ApJ, 247, 403
Kellermann K. I., Sramek R., Schmidt M. et al., 1989, AJ, 98, 1195
Komossa S., Mathur S., 2001, A&A, 374, 914
Kriss G., 1994, Adass, 3, 437
Kuraszkiewicz J., Wilfes B. J., Czerny B., Mathur, S., 2000, ApJ, 542, 692
Laor A., 2000, ApJ, 543, 111
Laor A., Fiore F., Elvis M., Wilkes B. J., McDowell J. C., 1997, ApJ, 477, 93
Leighly K. M., 1999, ApJS, 125, 297
Levenson N. A., Weaver K. A., Heckman T. M., 2001, ApJ, 550, 230
Mathur S., 2000, MNRAS, 314, 17
Mason K. O., Hassall B. J. M., Bromage G. E. et al., 1995, MNRAS, 274, 1194
Mason K. O., Puchnarewicz E. M., Jones L. R., 1996, MNRAS, 283, 26
Meyers K. A., Peterson B. M., 1985, PASP, 97, 734
Nagao T., Murayama T., Taniguchi Y., 2001, ApJ, 546, 744
Nagao T., Murayama T., Shioya Y, Taniguchi Y., 2002, ApJ, 575, 721
Osterbrock, D. E., 1989, Astrophysical of Gaseous Nebulae and Active Galactic Nuclei, Mill Valley CA: University Science Books
Osterbrock D. E., Pogge R. W., 1985, ApJ, 297, 166
Penston M. V., Robinson A., Alloin D. et al., 1990, A&A, 236, 53
Pogge R. W., 2000, NewAR., 44, 381
Pounds K. A., Allan D. J., Barber C. et al., 1993, MNRAS, 260, 77
Pounds K. A., Done C., Osborne J. P., 1995, MNRAS, 277, 5
Pounds K., Vaughan S., 2000, NewAR, 44, 431
Puchnarewicz E. M., Mason K. O., Siemiginowska A., Pounds K. A., 1995, MNRAS, 276, 20
Puchnarewicz E. M., Mason K. O., Cordova F. A. et al., 1992, MNRAS, 256, 589
Pye J. P., McGale P. A., Allan D. J. et al., 1995, MNRAS, 274, 1165
Reeves J. N., Turner M. J. L., 2000, MNRAS, 316, 234
Remillard R. A., Bradt H., V., Buckley D. A. H. et al., 1986, ApJ, 301, 742
Rodriguez-Ardila A., Binette L., Pastoriza M. G., Donzelli C. J., 2000, ApJ, 538, 581
Romano P., Mathur S., Turner T. J. et al., 2004, ApJ, 602, 635
Schinnerer E., Eckart A., Tacconi L. J., 1998, ApJ, 500, 147
Schneider D. P., Richards G. T., Fan X. T. et al., 2002, AJ, 123, 567
Schmidt M., Green R. F. ApJ, 1983, 269, 352
Shara M. M., Shara D. J., McLean B., 1993, PASP, 105, 387

Siebert J., Leighly K. M., Laurent-Muehleisen S. A. et al., 1999, A&A, 348, 678
Stephens S. A., 1989, AJ, 97, 10
Storey P. J., Zeippen C. J., 2000, MNRAS, 312, 813
Stirpe G. M., van Groningen E., de Bruyn A. G., 1989, A&A, 211, 310
van Groningen E., de Bruyn A. G., 1989, A&A, 211, 293
Vaughan S., Pounds K. A., Reeves J., Warwick R., Edelson R., 1999, MNRAS, 308, 34
Veilleux S., 1991, ApJ, 75, 357
Veilleux S., Osterbrock D. E., 1987, ApJS, 63, 295
Véron-Cetty M. -P., Véron P., Goncalves A. C., 2001, A&A, 372, 730
Vrtilek J. M., Carleton N. P., 1985, ApJ, 194, 106
Wandel A., 2000, NewAR, 44, 427
Whalen J., Laurent-Muehleisen S. A., Moran E. C., Becker R. H., 2001, A&AS, 199, 5001
Whittle M., 1985, MNRAS, 213, 33
Williams R. J., Pogge R. W., Mathur S., 2002, AJ, 124, 3042
Winkler H., 1992, MNRAS, 257, 677
Zamanov R., Marziani P., Sulentic J. W. et al., 2002, ApJ, 576, 9
Zhou H. Y., Wang T. G., 2002, Chin. J. Astron. Astrophys., 2, 501
Zhou H. Y., Wang T. G., Dong X. B., Zhou Y. Y, Li C., 2003, ApJ, 584, 147